Tree Physiology 42, 71–85
https://doi.org/10.1093/treephys/tpab091

Research paper

Temperature memory and non-structural carbohydrates mediate legacies of a hot drought in trees across the southwestern USA

Drew M. P. Peltier[1,2,12], Jessica Guo[3], Phiyen Nguyen[2], Michael Bangs[2], Michelle Wilson[2], Kimberly Samuels-Crow[1], Larissa L. Yocom[4], Yao Liu[5], Michael K. Fell[1], John D. Shaw[6], David Auty[7], Christopher Schwalm[8,9], William R.L. Anderegg[10], George W. Koch[2,11], Marcy E. Litvak[11] and Kiona Ogle[1,2]

[1]School of Informatics, Computing, and Cyber Systems, Northern Arizona University, Flagstaff, AZ 86011, USA; [2]Department of Biological Sciences, Northern Arizona University, Flagstaff, AZ 86011, USA; [3]Communications and Cyber Technologies, University of Arizona, Tucson, AZ 85721, USA; [4]Department of Wildland Resources and the Ecology Center, Utah State University, Logan, UT 84322, USA; [5]Geography and Environmental Sciences, Northumbria University, Newcastle upon Tyne, UK; [6]USDA Forest Service, Rocky Mountain Research Station, Ogden, UT 84401, USA; [7]School of Forestry, Northern Arizona University, Flagstaff, AZ 86011, USA; [8]Woods Hole Research Center, Falmouth, MA 02540, USA; [9]Center for Ecosystem Science and Society, Northern Arizona University, Flagstaff, AZ 86011, USA; [10]School of Biological Sciences, University of Utah, Salt Lake City, UT 84112, USA; [11]Department of Biology, University of New Mexico, Albuquerque, NM 87131, USA; [12]Corresponding author (dmp334@nau.edu)

Received January 21, 2021; accepted July 16, 2021; handling Editor Frederick Meinzer

Trees are long-lived organisms that integrate climate conditions across years or decades to produce secondary growth. This integration process is sometimes referred to as 'climatic memory.' While widely perceived, the physiological processes underlying this temporal integration, such as the storage and remobilization of non-structural carbohydrates (NSC), are rarely explicitly studied. This is perhaps most apparent when considering drought legacies (perturbed post-drought growth responses to climate), and the physiological mechanisms underlying these lagged responses to climatic extremes. Yet, drought legacies are likely to become more common if warming climate brings more frequent drought. To quantify the linkages between drought legacies, climate memory and NSC, we measured tree growth (via tree ring widths) and NSC concentrations in three dominant species across the southwestern USA. We analyzed these data with a hierarchical mixed effects model to evaluate the time-scales of influence of past climate (memory) on tree growth. We then evaluated the role of climate memory and the degree to which variation in NSC concentrations were related to forward-predicted growth during the hot 2011–2012 drought and subsequent 4-year recovery period. *Populus tremuloides* exhibited longer climatic memory compared to either *Pinus edulis* or *Juniperus osteosperma*, but following the 2011–2012 drought, *P. tremuloides* trees with relatively longer memory of temperature conditions showed larger (more negative) drought legacies. Conversely, *Pinus edulis* trees with longer temperature memory had smaller (less negative) drought legacies. For both species, higher NSC concentrations followed more negative (larger) drought legacies, though the relevant NSC fraction differed between *P. tremuloides* and *P. edulis*. Our results suggest that differences in tree NSC are also imprinted upon tree growth responses to climate across long time scales, which also underlie tree resilience to increasingly frequent drought events under climate change.

Keywords: asymmetry, Bayesian, Dendroecology, NSC, osmoregulation, recovery.

Introduction

Tree growth is a fundamental process driving forest productivity across forested ecosystems (Pan et al. 2011). The accumulation of tree-ring datasets has led to a surge in the use of tree-ring data to address questions related to the physiological basis of tree growth (Klesse et al. 2020) and the legacies of climatic extremes (e.g., drought) (Anderegg et al. 2015). More broadly, past work has investigated growth correlations with both recent and antecedent climate variables among species or sites to infer growth behaviors (e.g., Makinen et al. 2000, Sarris et al. 2007, Mazza and Manetti 2013, Bond-Lamberty et al. 2014, Marquardt et al. 2018, Liu et al. 2019). Perhaps because trees are long-lived organisms, with physiological inertia driving difficult to explain variation across their life-spans (Melvin and Briffa 2008, Esper and Frank 2009), large scale syntheses across forest ecosystems and continents have revealed new temporal complexities in tree growth responses to drought severity and frequency (Anderegg et al. 2015, Peltier et al. 2016, Schwalm et al. 2017, Peltier and Ogle 2019*a*, 2019*b*).

The lagged effects of climate (e.g., 'climatic memory'; Ogle et al. 2015) on tree growth are prevalent in semi-arid forests and woodlands (Peltier et al. 2018), systems in which trees experience highly variable climate conditions (Knowles et al. 2020). The mechanisms of climatic memory are not well understood, though physiological observations following climatic extremes such as drought hold promise. For example, cessation of 11 years of irrigation in *Pinus sylvestris* led to lagged declines in canopy and leaf area metrics as well as radial growth over 4 years post-irrigation (Zweifel et al. 2020). Across temperate forests, precipitation extremes lead to multi-year perturbations to the sensitivity of tree growth to climate (Anderegg et al. 2015, Peltier and Ogle 2020) with implications for terrestrial carbon fluxes (Babst et al. 2014, Nehrbass-Ahles et al. 2014, Schwalm et al. 2017). These effects have been shown to be most prevalent in conifers in semi-arid regions (Anderegg et al. 2015, Peltier et al. 2016). While not a major focus of regional tree-ring syntheses, there is also large variation in climatic memory and drought legacies across sites, with implications for forest resilience to changing frequency and severity of temperature and moisture extremes across the landscape (Williams et al. 2020). Yet, the drivers of this variation are also poorly studied, as studies (e.g., Anderegg et al. 2015, Peltier et al. 2016) often focus more on quantifying average responses across large regions (e.g., the western USA) or taxonomic groups (e.g., conifers). Quantifying and exploring the drivers of variability in climatic memory, as well as the differences among species, can lend insight to the underlying physiological mechanisms—ultimately necessary if we are to improve our ability to predict tree growth and resilience under future climate change and drought.

Despite widespread recognition and interest in drought legacies (perturbed growth-climate responses) and lagged effects of climate on tree growth (under normal climate conditions, i.e., non-perturbed), the physiological mechanisms of these effects are rarely the focus of experimental observation (reviewed in Kannenberg et al. 2020, Peltier and Ogle 2020; but see von Arx et al. 2017, Zweifel et al. 2020). The multi-year persistence of conifer needles, which results in slow canopy area dynamics, was proposed as an initial explanation for lagged climate responses of conifers (e.g., LaMarche Jr and Stockton 1974). To explain multi-year drought legacies, more recently proposed mechanisms include lasting hydraulic damage, particularly if trees are large enough that whole-tree conductance requires multiple years to recover (demonstrated in Trugman et al. 2018). Similarly, transient depletion or changes in allocation of non-structural carbohydrates (NSC) might also explain slow recovery following drought (Peltier et al. 2016), particularly if trees must remobilize very old NSC pools, as has been observed in some mature trees (Carbone et al. 2013). Post-drought allocation of NSCs has been shown to be biased belowground in one conifer species (Hagedorn et al. 2016), but aboveground in multiple species in the eastern USA, leading to no change in productivity following drought (Kannenberg et al. 2019). The most often cited function of NSC storage is to sustain tree functions in periods when carbon demand exceeds supply, buffering trees from stress (Dietze et al. 2014, Kozlowski 1992). Thus, we may expect that NSCs serve to decouple tree growth from cotemporaneous climatic variability, giving rise to climatic memory (von Arx et al. 2017).

In this study, we quantify variation in both the length and temporal pattern of climatic memory in dominant tree species across the southwestern USA. We explore how climatic memory of tree growth is related to NSC through multiple approaches. We leverage a combined tree-ring and snapshot NSC dataset across a network of 22 sites in the southwestern US, encompassing three dominant tree species: *Pinus edulis, Juniperus osteosperma* and *Populus tremuloides*. We used these data to address the following questions: (Q1) How does the temporal pattern of the climatic memory of tree growth vary across ecologically sampled sites (Nehrbass-Ahles et al. 2014) in the southwestern USA? Following a severe, hot regional drought in 2011–2012 (Williams et al. 2013, Cook et al. 2014, Anderegg et al. 2019, Figure 1), we ask: (Q2) Is regional variation in drought legacies (post-drought perturbed growth-climate response) explained by the length of climatic memory (average lag in growth response to climate across the record)? For example, do trees with longer climatic memory also experience longer legacies of drought, or conversely, does longer climatic memory buffer trees from the impacts of drought, resulting in reduced recovery times? Because we also sought to understand potential mechanisms underlying temporal properties of tree growth-climate relations

across species in the Southwest, we also ask: (Q3) Is there a role of NSC in explaining the length of climatic memory and/or the severity of drought legacies with respect to tree growth?

While growth time-series are easily obtained from tree core collections, long time-series of physiological processes are limited (Pérez-Ramos et al. 2010, Vacchiano et al. 2017). Without time-series of physiological data, physiological measurements are essentially a 'snapshot' with respect to the time-scales of tree growth processes. However, while variation in NSC concentrations may reflect recent climate (e.g., precipitation surpluses or deficits; Dietze et al. 2014), variation across individuals or species may also be partially explained by species traits (Godfrey et al. 2020)—perhaps reflecting NSC storage capacity and wood anatomy (Hoch et al. 2003)—or acclimation to prevailing site climate conditions (Piper et al. 2017). As we have recently explored how NSC concentrations in this network respond to moisture stress at varying time scales (Peltier et al. 2020), we focus here on these other sources and drivers of NSC variation. Thus, in addressing Q3, we hypothesize that trees within a species maintaining relatively higher NSC concentrations will have relatively longer climatic memory, and therefore exhibit comparatively minor (small) legacies following the 2011–2012 drought.

Methods

Study sites and climate data

We sampled *P. tremuloides* (aspen), *P. edulis* (piñon) and *J. osteosperma* (juniper) across 22 sites (11 piñon-juniper and 11 aspen sites) in Utah, Colorado, New Mexico and Arizona. The sites spanned a broad range of mean temperature and precipitation conditions (Figure 1). Sampling sites were located in close proximity to Forest Inventory and Analysis (FIA) permanent sample plots. Information from the FIA database was used to help identify sites; for example, sites were chosen based on criteria such as species composition, stand density and accessibility (public ownership), and excluded if potentially impacted by a disturbance, such as wildfire, that occurred since the last FIA measurement period.

Sampling for NSC concentrations took place twice at each site during 2016 (pre- and mid-monsoon season, defined below), and tree core sampling took place in summer 2017. Tree-ring widths (described below) were related to monthly precipitation (P) and temperature (T) data obtained from the PRISM group (PRISM climate group 2004), and to self-calibrating Palmer Drought Severity Index (PDSI, hereafter D) obtained from the West Wide Drought Tracker (Abatzoglou et al. 2017); all climate datasets are 4 km spatial resolution.

Tree coring and processing

We collected at least two replicate tree cores from 15–17 trees per site in summer 2017 to measure growth (i.e., ring widths). We sampled relatively 'ecologically' (Nehrbass-Ahles et al. 2014), that is, we aimed to select fairly representative trees in each site, spanning different sizes and canopy positions. Towards the same goal, we did not exclude trees with fire scars, up to moderate canopy dieback, or common aspen conks (*Phellinus tremulae*), though we only selected piñon and juniper trees with single stems. Tree cores were collected with 5.15 mm Haglof (Sweden) or Jim-Gem (Forestry Suppliers Inc.) increment borers as close to the ground (base) as possible, and perpendicular to hill slopes. Cores were sometimes collected above breast height in aspen to avoid collecting cores with substantive heart-rot, or not parallel to hill slopes in piñon or juniper trees with irregularly shaped or partially dead boles. Coring height, diameter at coring height and diameter at breast height (DBH, cm) were recorded for all trees. We attempted but did not always succeed in coring through the pith (e.g., in very old trees or irregularly shaped boles). Some piñon and juniper trees cored were over 300 years old, while aspen trees tended to be <100 years old.

Tree cores were processed following standard methods (Fritts and Swetnam 1989): cores were air dried, mounted and sanded with increasingly fine-grained sand-paper. Cores were then visually crossdated and measured on a Velmex tree-ring measurement system (Bloomfield, NY). Visual crossdating was verified with COFECHA, and problematic cores were re-dated or excluded from subsequent analyses. Juniper cores from some sites proved extremely difficult to crossdate, and thus ring widths at only four sites were ultimately included in this analysis for juniper (Table 1). Tree-ring widths were detrended for age effects for the entire length of each core using a modified negative exponential or flat line using the dplr package (Bunn 2008) in R Core Team (2019). Thus, increasing trends in ring width with age were considered to be ecological (not an actual age effect) and were not removed. This detrending resulted in tree-level ring width indices (hereafter 'RWI'), with mean RWI equal to 1 representing 'average' growth. To align this, the climate data, we excluded all RWI observations preceding 1899 (4 years after the beginning of PRISM climate data, Figure S1 available as Supplementary data at *Tree Physiology* Online).

NSC sampling

To capture maximum seasonal variability in NSC, sites were visited between DOY 158–180 (June 6–28; pre-monsoon) and 229–261 (August 16-September 17; mid-monsoon) in 2016, capturing the hot-dry period preceding the onset of the North American monsoon (NAM) and the comparatively cool and wet period at the height of NAM activity, respectively. We sampled a subset (five) of the 15–17 study trees (subsequently cored in 2017, described above) per species per site for NSC measurements. We collected leaf (or needle) and twig tissues using clippers or pole pruners in mid-afternoon from three sides of each tree canopy, and subsequently processed

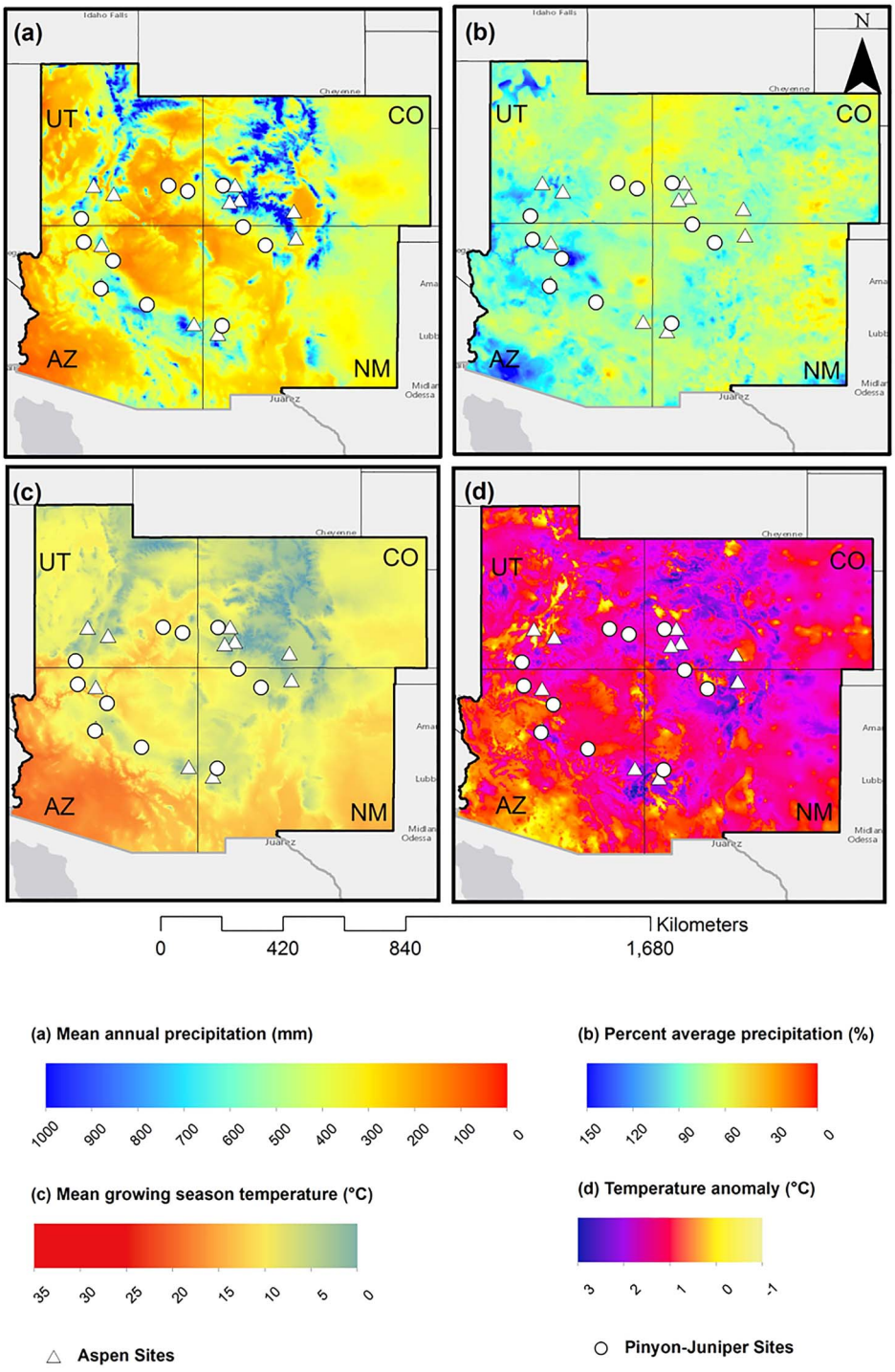

Figure 1. Climate summaries in the southwestern USA show the imprint of the hot 2011–2012 drought across the tree-ring network where (a) MAP for the 30-year period 1981–2010, (b) water-year (October–September) precipitation anomaly (as percent of MAP) during the 2011–2012 drought, (c) mean growing season (April–October) temperature (1981–2010) and (d) growing season temperature anomaly (as deviation from mean growing season temperature) during the 2011–2012 drought. Warmer colors indicate drier and/or warmer conditions. Climate data are from PRISM climate group. The 22 study sites are indicated by the symbols (triangles = aspen sites; circles = piñon-juniper sites). States are UT = Utah, CO = Colorado, AZ = Arizona and NM = New Mexico. Site-specific climate anomalies are summarized in Table 1.

these tissue samples according to standard methods (Quentin et al. 2015, Landhäusser et al. 2018): tissue samples were immediately frozen on dry ice for transport to lab facilities in Flagstaff, Arizona, USA. Transport times ranged from 1 to 6 days (most often a maximum of 2–3 days). For piñon, we separated twigs and needles according to annual cohorts, and analysis

Table 1. Site locations, names, elevations (m a.s.l.), summary climate information, and description of the numbers of trees sampled and cores successfully crossdated; summary tree-ring statistics (sensitivity) are also included. MAP (mm) and mean annual temperature (MAT, °C) are calculated from over 30 years (1981–2010) of the PRISM climate data. Series range describes the years spanned by the dated tree-ring series at a given site. Sensitivity is the 'mean sensitivity' obtained from COFECHA. Site abbreviations are defined in Figure 1, species are a = aspen, P = piñon and J = juniper. 2011–2012 climate anomalies are also shown in Figure 1b and d

State	Site	Location	Elevation (m)	MAP (mm)	MAT (°C)	2011–12 MAP anomaly (%)	2011–12 MAT anomaly (°C)	Trees	Cores	Series range	Sensitivity
AZ	A1	35.16, −112.17	2157	606.58	9.69	83	1.8	15	30	1951–2016	0.48
AZ	P1	36.50, −112.73	1680	320.66	12.7	87	1.0	9	17	1930–2016	0.534
AZ	A2	36.41, −112.17	2781	821.65	6.1	72	1.1	14	26	1933–2016	0.359
AZ	P2	35.92, −111.83	1937	347.84	9.6	91	0.6	15	30	1952–2016	0.317
AZ	A3	33.97, −109.32	2845	660.81	5.95	76	2.1	15	30	1968–2016	0.393
AZ	P3	35.06, −112.21	1896	538.72	11.1	87	1.9	14	28	1947–2016	0.36
AZ	P4	34.57, −110.78	2001	400.84	10.46	86	0.9	15	30	1916–2016	0.456
CO	A4	37.74, −108.22	2791	681.51	4.2	81	1.8	15	29	1951–2016	0.311
CO	A5	37.46, −106.24	2714	501.38	3.57	67	1.9	12	25	1935–2016	0.46
CO	A6	37.81, −107.91	3147	932.1	1.9	74	1.9	15	30	1944–2016	0.229
CO	P5	38.24, −108.43	1962	351.03	9.36	70	1.4	15	30	1890–2016	0.451
CO	J1	38.24, −108.43	1962	351.03	9.36	70	1.4	15	30	1850–2016	0.673
CO	A7	38.26, −108.05	2915	645.67	4.39	75	1.5	15	30	1962–2016	0.304
NM	P6	36.97, −107.81	2069	391.15	9.85	72	2.5	14	26	1898–2016	0.45
NM	J2	36.97, −107.81	2069	391.15	9.85	72	2.5	13	23	1883–2016	0.527
NM	A8	36.64, −106.18	2825	552.12	5.25	71	2.2	15	30	1965–2016	0.433
NM	P7	33.92, −108.46	2140	360.11	9.13	90	1.0	15	30	1951–2016	0.432
NM	P8	36.40, −107.12	2246	372.05	7.85	86	1.1	14	27	1904–2016	0.45
NM	J3	36.40, −107.12	2246	372.05	7.85	86	1.1	6	11	1907–2016	0.736
NM	A9	33.68, −108.58	2853	372.05	8.07	71	2.2	15	30	1969–2016	0.411
UT	A10	38.00, −111.80	2944	641.54	3.93	91	0.9	15	33	1937–2016	0.225
UT	P9	38.08, −109.52	2019	314.26	10.56	66	1.6	14	26	1890–2016	0.51
UT	A11	38.25, −112.42	2941	838.98	4.08	84	1.3	15	30	1931–2016	0.258
UT	P10	37.22, −112.80	1827	390.25	11.72	84	1.9	15	31	1860–2016	0.424
UT	J4	37.22, −112.80	1827	390.25	11.72	84	1.9	15	27	1830–2016	0.569
UT	P11	38.25, −110.11	1949	237.4	11.49	74	1.0	14	28	1910–2016	0.63

here focused on the youngest cohorts (formed in 2016). After transport, samples were microwaved, oven dried for 72 h at 60°C, and subsequently frozen at −20°C until analysis. We used a phenol–sulfuric acid method to extract NSCs and analyzed in-house tissue- and species-specific standards with each run. See Methods S1 for full reporting of NSC methods. For this study, NSC concentrations for the two key fractions, (soluble) sugars and starch, were each aggregated into means for each combination of site and species for a given tissue (leaf or twig) and sampling period (pre-monsoon or mid-monsoon) to be comparable to site-level estimates of climatic memory and drought legacies (see *implicit and additive roles of NSC*). Further information on the NSC dataset is also available in Peltier et al. (2020).

Tree growth (RWI) model

Following Peltier et al. (2018), we analyzed the tree-level RWI data via a hierarchical mixed effects model based upon the stochastic antecedent modeling (SAM) framework (SAM; Ogle et al. 2015, Ryan et al. 2015). A description of the theory and motivation underlying the modeling framework are given in (Ogle et al. 2015), additional model description is provide in Methods S2, and full model code in Methods S3. The key concept of the SAM framework is the antecedent covariates, X^{ant}, themselves weighted averages of past monthly climate values, X (here, precipitation [P], temperature [T] or PDSI [D]), with weights, $w_{l,m,st,v}$, subscripted by years l into the past, month m ($m = 1, 2, \ldots, 12$ for January, February, ..., December), site-species combination st and covariate v (i.e., P, T or D); hence,

$$X^{ant}_{st,y} = \sum_{l=0}^{4} \sum_{m=1}^{12} w_{l,m,st,v} \cdot X_{y-l,m,st} \quad (1)$$

We extended the weights to 4 years into the past ($l = 0, 1, \ldots, 4$ for current year, previous year, ..., 4 years prior) relative to year y, encompassing 5 years including the year of ring formation. Thus, since the PRISM dataset starts in 1895, 1899 is the first year of growth (RWI) data considered in the model. The weights (w) used to construct these antecedent covariates are stochastic parameters that are estimated (see Methods S2),

allowing inference on both the length and temporal pattern of climatic memory (see *Calculated quantities*) of tree growth responses to climate (Peltier et al. 2018) across our study sites and species.

Then, we fit a simple linear model to the RWI data, conditional on the antecedent climate covariates (P^{ant}, T^{ant} and D^{ant}; Eqn 1). This *tree growth model* regresses RWI on antecedent climate covariates of precipitation (P^{ant}), temperature (T^{ant}) and PDSI (D^{ant}), and includes an additive AR1 term (i.e., previous-year RWI). Note that here, the effect of D^{ant} represents an interaction between P^{ant} and T^{ant}, as the PDSI product we use is derived directly from PRISM precipitation and temperature data (Peltier and Ogle 2019*a*, 2019*b*). We also include two-way interactions between precipitation and PDSI ($P^{ant} \times D^{ant}$) and between temperature and PDSI ($T^{ant} \times D^{ant}$) to capture non-linearity in the climate responses. The intercept term, the main effects of P^{ant}, T^{ant}, D^{ant} and previous-year RWI, and the two 2-way interaction effects are all estimated uniquely for each tree, and these tree-level effects parameters are modeled hierarchically around overall site-species effects (e.g., see Peltier et al. 2018).

The aforementioned *tree growth model* was fit to the RWI data spanning 1899–2012 (RWI for 2013 and beyond were withheld for evaluating drought legacies, see next section). The model was implemented in a hierarchical Bayesian framework in JAGS (Plummer and others 2003) through R Core Team (2019) via the package 'rjags' (Plummer 2013), following standard methodology, as described in previous applications of the SAM model to tree-ring data (e.g., Peltier et al. 2018).

Quantifying climatic memory and drought legacies

We evaluated two components of climatic memory (*sensu* Ogle et al. 2015): (1) the temporal pattern of memory and (2) the length of memory. First, the temporal pattern of memory is inferred directly from the temporal pattern of the estimated monthly weights (w, Eqn 1). Note that the temporal pattern of memory for PDSI is somewhat difficult to resolve, given inherent autocorrelation; however previous work with this model (Peltier and Ogle 2019*a*, 2019*b*) has shown PDSI to be the best choice of covariate, both because it represents an interaction between P^{ant} and T^{ant} (see *tree growth model*), and improves computational behavior of the model. For the length of memory, we used the weights to quantify the time into the past at which 50% of the influence of a given climate variable has been reached for a given site or species; that is, we identified the month (into the past) at which the cumulative sum of the monthly weights exceeds 0.5 (e.g., Ogle et al. 2015). Conceptually, this measure quantifies the antecedent window of time necessary to capture 50% of the climate (e.g., precipitation) information relevant to growth (according to the weights). We refer to this quantity as P_{50}, T_{50} and D_{50} for precipitation, temperature and PDSI, respectively. We also estimated X_{75} and X_{90} (for X = P, T or D), which represent the months into the past where the cumulative weights equal 75% and 90%, respectively. Calculations of X_{50}, X_{75} and X_{90} were performed within the JAGS simulation model, allowing parallel estimation of the associated uncertainty in these indices of the length of climatic memory.

Again, we withheld RWI observations from 2013 to 2016 from the model fitting and parameter estimation stage and used these data to calculate drought legacies. The AR1 covariate (previous-year RWI) was propagated forward for the years 2013–2016. That is, the 2013 RWI prediction was informed by observed RWI in 2012, whereas the 2014 RWI prediction was informed by predicted RWI in 2013 (the previous year's RWI prediction). Thus, we quantified the drought legacies for each tree following the 2011–2012 drought—which was severe (Williams et al. 2013, Cook et al. 2014)—as the difference (error) between observed RWI (RWI^{obs}) and predicted RWI (RWI^{pred}); thus, the drought legacy effect, $d_{y,tr}$, in year y (for years 2012–2016) for tree tr is defined as:

$$d_{y,tr} = RWI^{obs}_{y,tr} - RWI^{pred}_{y,tr} \quad (2)$$

Drought legacies (d) were estimated at the tree-level and then averaged across trees to obtain site-level legacies for each year (d^*_{yr}). We assume that legacies (d) that are similar across the tree ring network are thus indicative of the impact of the 2011–2012 drought. While numerous other factors may influence tree growth–climate sensitivity (Peltier and Ogle 2020), drought is the most likely driver of regionally coherent perturbations to tree growth–climate sensitivity, particularly in the southwestern USA (Anderegg et al. 2015).

Implicit and additive roles of NSC

We explored potential relationships between climatic memory and NSC concentrations measured in 2016 in these legacies, and the implicit role of NSCs in climatic memory, using a two-step linear regression process (Methods S4). First, to select the indices of memory length most important in driving site-level drought legacies, we regressed annual legacies (i.e., d^*_{yr} for 2012–2016) on the different indices of memory length (P_{50}, P_{75}, ... and D_{90}). To select the most important relationships, we only focus on the linear regressions that were significant ($P < 0.05$) and for which the coefficient of determination (R^2) was greater than 0.10.

Next, to understand the implicit versus additive roles of NSC pools in drought legacies, we subsequently only focused on the memory indices that were deemed important for understanding drought legacies (above), implementing two types of regressions. First, to understand the 'implicit' roles of NSC, we regressed these memory length indices (e.g., $T_{75,st}$, among others) directly on site-level mean NSC concentrations to test whether memory may be related to variation in NSC pools across sites; e.g., for site st, NSC fraction fr and date (pre-monsoon or mid-monsoon) m, we regressed $T_{75,st}$ on $NSC_{fr,st,m}$,

and so forth for the other important memory length indices. These relationships ('implicit' effects) describe the effect of variation in NSC concentrations across sites upon variation in climate memory indices relevant to drought legacies. Second, we evaluated the 'additive' roles of NSC by expanding the original regressions of drought legacies to include both the previously identified important memory indices and site-level mean NSC concentrations; e.g., we regressed d^*_{yr} on $T_{75,st}$ and $NSC_{fr,st,m}$. These relationships ('additive' effects) describe the additional variation in drought legacies explained by NSC when also including effects of memory indices. These analyses were all performed in base R, and are further described, along with the workflow of all prior steps (fitting tree growth model, memory indices, drought legacies) leading up to these analyses, in Methods S4.

Results

We successfully crossdated and measured 717 (~73%) of the 984 cores collected (Figure S1 available as Supplementary data at *Tree Physiology* Online). This subset represented 96% of the aspen, 90% of the pinyon and 30% of the juniper cores. Sites successfully crossdated and used in subsequent analyses are given in Table 1. Overall fit of the *tree growth model* was moderately high (coefficient of determination, $R^2 = 0.64$). The model fit was higher for piñon ($R^2 = 0.67$) and juniper ($R^2 = 0.67$) and relatively lower for aspen ($R^2 = 0.58$), reflecting lower mean sensitivity in aspen, both in the crossdating statistics (Table 1), and with respect to sensitivity to precipitation and temperature (Figure 2a and b).

Dendroecological variation in climate responses and climatic memory

Responses to climate differed among species, but also showed strong variation across the study region (Figure 2). Tree RWI responded positively to antecedent precipitation (P^{ant}) across the study region with the exception of aspen trees at site A6, the highest elevation site with the highest mean annual precipitation (MAP, Figure 2a). Responses of RWI to antecedent temperature (T^{ant}) could be positive or negative in aspen, but were primarily negative in piñon and juniper (at the four sites we were able to crossdate, Figure 2b). Except for site A6, responses to antecedent PDSI (D^{ant}) were negative or non-significant (Figure 2c). The D^{ant} effects are consistent with previous applications of this modeling framework using the same climate data products, where D^{ant} is equivalent to an interaction between precipitation and (negative) temperature (Peltier and Ogle 2019*a*, 2019*b*). Thus, negative D^{ant} responses suggest higher precipitation sensitivity under warmer temperatures, consistent with evidence that VPD was a major component of the 2012 drought event (Williams et al. 2013, Figure 1d). Given the aforementioned interpretation, the $P^{ant} \times D^{ant}$ and

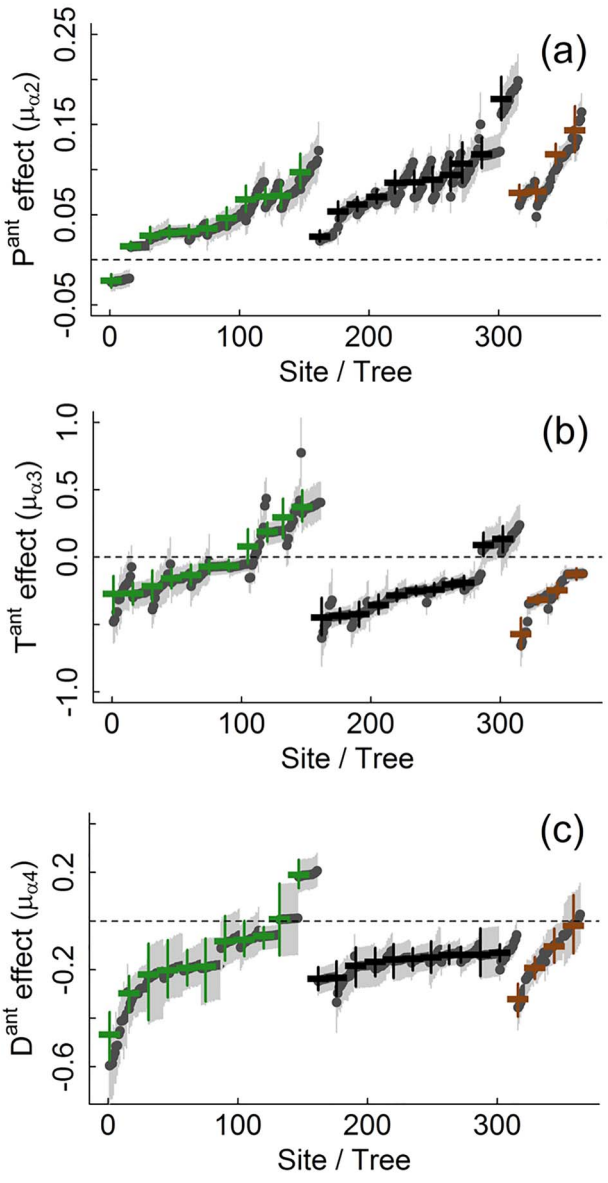

Figure 2. Posterior means and 95% central credible intervals (CI) for the site-level climate effects indicate strong site- and tree-level variation in climate sensitivity across the ecologically sampled tree-ring network. Climate effects are shown for: (a) antecedent precipitation (P^{ant}), (b) antecedent temperature (T^{ant}) and (c) antecedent drought or PDSI (D^{ant}) for each aspen (green triangles and lines), piñon (black triangles and lines) and juniper (brown triangles and lines). The mean ± 95% CIs for the tree-level (a-c) effects (dark gray points and light gray vertical lines) are shown behind the site-level effects (darker, colored symbols). Within species and site, all effects are sorted according to magnitude and thus a particular tree or site in one panel does not directly align with another panel. The horizontal dashed lines indicate the zero line, and 95% CIs that overlap this line denote non-significant effects. $P^{ant} \times D^{ant}$ and $T^{ant} \times D^{ant}$ interactions and AR1 effects are reported in Figure S2 available as Supplementary data at *Tree Physiology* Online.

$T^{ant} \times D^{ant}$ interactions represent small curvature in the effects of P^{ant} and T^{ant} on growth; these interaction effects were variable across sites and species, including positive, negative and non-significant effects (Figure S2d and e available as

Supplementary data at *Tree Physiology* Online). The site-level AR1 effects were largest for piñon (posterior mean ± sd: 0.45 ± 0.14) and juniper (0.48 ± 0.07) and considerably smaller for aspen (0.27 ± 0.13) (Figure S2f available as Supplementary data at *Tree Physiology* Online). Unlike the climate effects, the within-site variation in AR1 effects was comparable to among-site variation in AR1 effects (Figure S2f available as Supplementary data at *Tree Physiology* Online).

Across species, there was also notable variation in the temporal pattern of the climate response (based on the monthly weights, $w_{l,m,st,v}$) across sites (Figure 3). Mean trends in monthly weights also showed clear differences across species, particularly for the effects of P^{ant} (Figure 3a). Consistent with the longstanding use of piñon and *Juniperus* spp. species in dendrochronology, weights in these species were highly peaked (Figure 3a) and concentrated on the period between the previous fall through the current growing season (previous September to current July), a pattern also typical of other Southwest conifers (Figure 3a, Peltier et al. 2018). The temporal pattern was notably more diffuse in aspen, showing greater reliance on antecedent precipitation conditions 1 and 2 years prior to the year of ring formation. For aspen, defined peaks of importance weight associated with P^{ant} also occurred during previous late summer periods 1 and 2 years prior to the year of ring formation (lags of 16–19 and 29–30 months, Figure 3a).

The temporal patterns of antecedent temperature responses were more similar across species and more diffuse compared to the antecedent precipitation weights. Though, there was a trend for the temperature importance weights to be concentrated (higher) during the early and late growing season of the year of or year prior to ring formation (Figure 3b). The weights also showed comparatively lower importance of winter temperature conditions across species (Figure 3b). Again, D^{ant} represents an interaction between P^{ant} and T^{ant}; the weights for D^{ant} show that this effect (amplified precipitation sensitivity during warmer periods) was most important during the warm and dry pre-monsoon periods, and this pattern is particularly apparent for piñon (19-month lag, Figure 3c).

Consistent with the temporal patterns described by the weights (Figure 3), the length of precipitation memory was longest in aspen compared to the other two species (Figure 4a). In particular, P_{50} was ~8 months longer and P_{75} was ~7 months longer in aspen compared to piñon, with larger differences when compared to juniper (Figure 4a). Memory in juniper was similar or shorter than in piñon, but we hesitate to compare given that means for juniper only represent four sites. Temperature memory length was fairly similar across species (Figure 4b), but PDSI memory length was somewhat longer in aspen, particularly with respect to D_{75} (~8 months longer in aspen than piñon; Figure 4c). Temperature and PDSI memory length in juniper were again somewhat shorter than in piñon (Figure 4b and c).

Legacies following the 2011–2012 drought

Trees of all three species grew ~50% less than was predicted by the model following the 2011–2012 drought (drought legacies were negative, Figure S3 available as Supplementary data at *Tree Physiology* Online). That is, tree responses to climate were altered by the 2011–2012 drought event in ways not captured by the fitted model, despite the model having included the effects of antecedent climate. For comparison, 2002 was another extreme regional drought, and data for this drought was included in model fitting. In the 4 years following 2002, average prediction error (legacy) magnitude across species was ~0.07, around 1/5 of the magnitude of the errors following 2012 (Figure S3 available as Supplementary data at *Tree Physiology* Online), and was not consistent in sign (overall mean 0.005 ± 0.30). Again, prediction error was smaller for the 2002 drought because the data associated with this event were included in model fitting, suggesting some characteristics of the 2012 drought were unique, or that the forward predictive power of the model is somewhat limited. Notably, species-level (mean of d^*_{yr}) legacies in juniper were similar in magnitude to the other two species, in contrast to previous studies finding little evidence of drought legacies in the *Cupressaceae* (Anderegg et al. 2015, Peltier et al. 2016).

Contrasting roles of climate memory in drought responses

Variation in the magnitude of drought legacies (d^*_{yr}) across sites was highly correlated with indices of memory (Table 2). Perhaps unexpectedly however, legacies were unrelated to variation in precipitation memory. Instead, drought legacies were more strongly related to variation in temperature and PDSI memory, but the sign of these relationships was opposite for aspen and piñon (Table 2). For example, the drought legacies (d^*_{yr}) in aspen were negatively correlated with memory length indices of temperature and PDSI, indicating more severe (more negative) legacies at aspen sites with longer climate memory (Table 2). In contrast, legacies were positively correlated with memory length indices of temperature and PDSI in piñon, indicating smaller (less negative) legacies at piñon sites with longer climate memory.

Memory and legacies are strongly related to NSC concentrations

We found strong relationships between climate memory length and NSC concentrations measured in 2016, especially with respect to twig NSC pools (*implicit effects*, Figure S4 available as Supplementary data at *Tree Physiology* Online). In aspen, sites with longer PDSI memory also had higher twig sugar concentrations in the pre-monsoon (R^2 = 0.43, respectively, Figure 5a). Piñon at sites with longer memory of temperature or PDSI tended to have lower twig starch concentrations but higher leaf and twig sugar concentrations (e.g., Figure 5b);

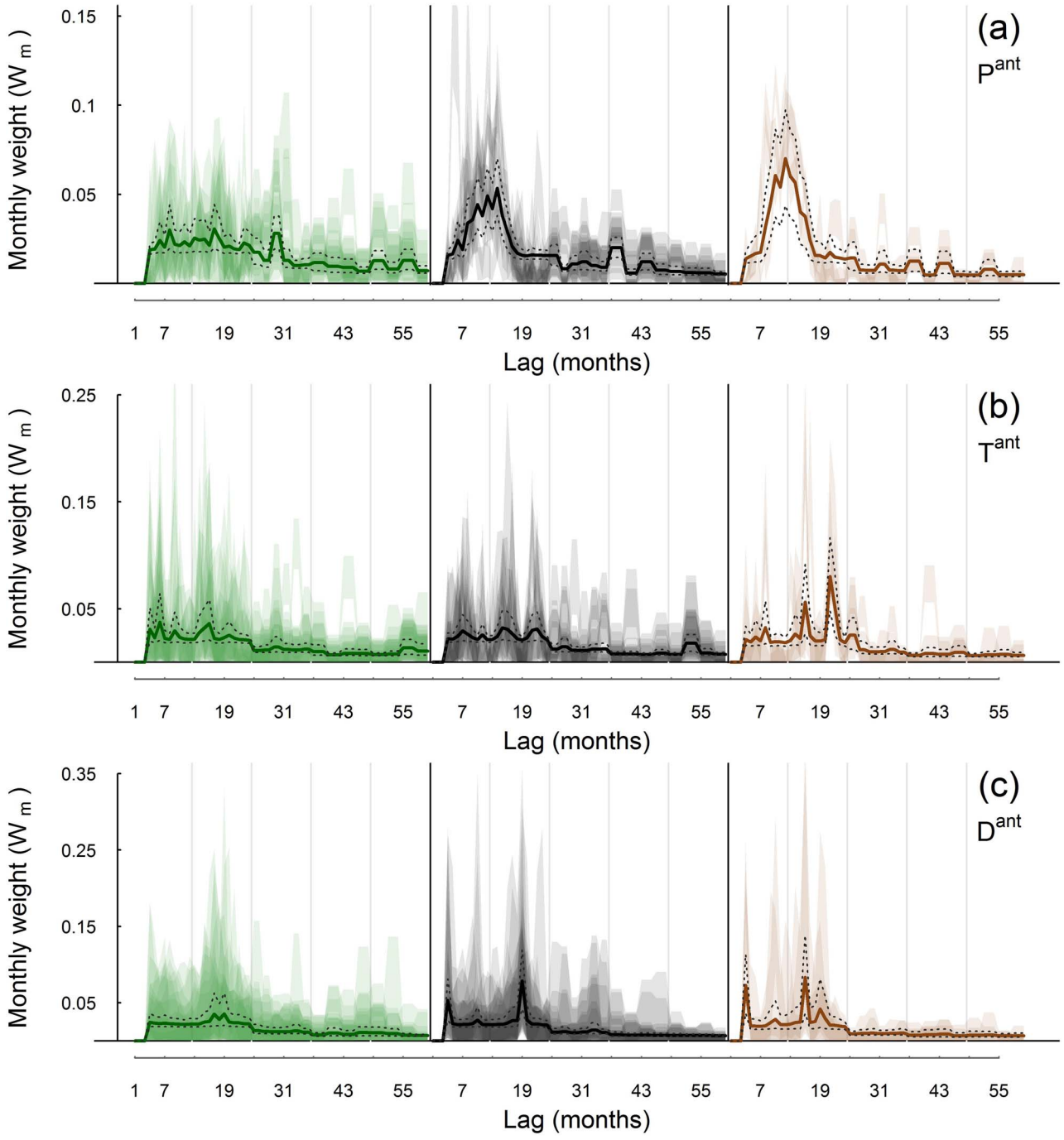

Figure 3. Patterns of climatic memory in piñon and juniper show peaked importance during the year of ring formation and the year prior, but climate memory in aspen is more diffuse over antecedent time. The thick lines show the posterior means and 95% central CIs of species-level monthly weights (w, see Eqn 1) corresponding to (a) antecedent precipitation (P^{ant}), (b) antecedent temperature (T^{ant}) and (c) antecedent drought or PDSI (D^{ant}) for aspen (green lines and green dashed lines), piñon (black lines and black dashed lines) and juniper (brown lines and brown dashed lines). Species-level means and 95% CIs are overlaid on the 95% CI's of site-level monthly weights ($w_{l,m,st,v}$) for aspen (green shading), piñon (gray shading) and juniper (brown shading). Vertical gray lines separate calendar years, and lag (months) is defined such that lag = 1 is December of the year of ring formation and lag = 60 is January 4 years prior to the year of ring formation.

these relationships were also fairly strong (R^2 = 0.32–0.64, Figure S4 available as Supplementary data at *Tree Physiology* Online). However, NSC concentrations (again only in twigs) were also directly related to drought legacies (d^*_{yr}) when considered as additional covariates in regressions of the drought legacies on climate memory length (*additive effects*), and these regressions led to fairly high total R^2 values. For example, at aspen sites where trees had higher twig starch concentrations, trees grew more than expected during the drought year, but had larger (more negative) drought legacies 2–4 years post-drought

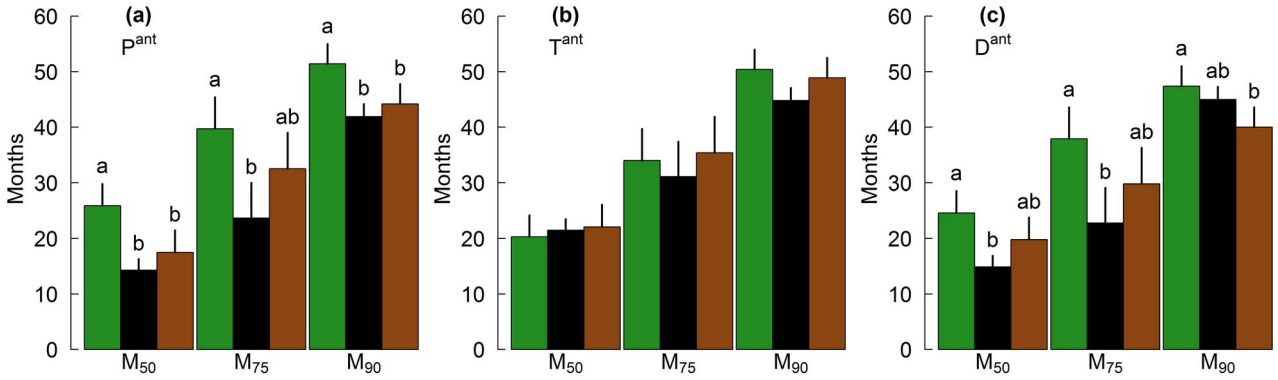

Figure 4. Climatic memory is longest in aspen, summarized here as indices of memory length (species mean ± sd) for (a) antecedent precipitation (p^{ant}), (b) antecedent temperature (T^{ant}) and (c) antecedent drought or PDSI (D^{ant}). The color of the bars and lines denote species: Aspen (green), piñon (black) and juniper (brown). Lowercase letters denote significant differences ($P < 0.05$, Dunn test following Kruskal-Wallis test) among species for a particular memory length index (e.g., M_{50}, M_{75} or M_{90}).

Table 2. Sign (shading) and strength (R^2) show opposite influences of memory length (M^{50}, M^{75} or M^{90}, for M = P for precipitation, T for temperature and D for drought or PDSI) on drought legacy severity (d^*_{201X}; predicted – Observed RWI for year 201X = 2013, 2014, 2015 or 2016) in aspen and piñon; but variation in precipitation memory length is unrelated to variation in drought legacy severity. Range of observed coefficients of determination (R^2) between annual drought legacies (d^*_{201X}) and memory length indices are reported for each recovery year (2013–2016) and covariate (P, T, PDSI). Shading indicates sign, where orange (blue) shading denotes negative (positive) correlations among memory length (P^{50}, …, D^{90}) and drought legacy magnitude. For example, because drought legacies are negative, here, negative (positive) correlations indicate more severe (less severe) drought legacies with longer climate memory

Aspen	P^{50-90}	T^{50-90}	D^{50-90}
d^*_{2013}	–	0.33	–
d^*_{2014}	–	–	–
d^*_{2015}	–	0.37	0.34
d^*_{2016}	–	–	0.32–0.41
Piñon	P^{50-90}	T^{50-90}	D^{50-90}
d^*_{2013}	–	0.35–0.49	–
d^*_{2014}	–	0.43–0.74	0.38
d^*_{2015}	–	0.42–0.61	–
d^*_{2016}	–	0.48–0.5	–

(Figure 5c). In piñon, higher twig sugars were associated with larger (more negative) drought legacies during the year after drought (Figure 5d).

Discussion

Using ecologically sampled tree-ring data for three species across 22 sites in the southwestern USA, we quantify site and species variation in the memory length of tree growth responses to climate (Figure 3). We show that site-to-site variation in memory and legacies of the 2011–2012 drought were each strongly related to 2016 NSC concentrations (Figure 5), despite that these do not represent the amount of NSCs available to trees during the actual drought event or subsequent recovery (discussed below). Complex variation across individuals and populations in the climate sensitivity of tree growth is ubiquitous (e.g., Pederson et al. 2020), but it is uncommon to quantify variation among populations in the temporal lags of the growth responses to climate, that is, variation in the temporal pattern (Figure 3) and length (Figure 4) of memory (Ogle et al. 2015). While patterns emerging at the species level (across all sites) match expectations of tree growth responses to climate, we also found evidence for large among-site variability (Figure 3). For example, patterns in precipitation memory in piñon and juniper align with those reported in dendrochronological studies and datasets (e.g., Fritts et al. 1965, Peltier et al. 2018), revealing a strong response to prior winter precipitation (Figure 3). However, it is also clear that individual piñon sites may support relatively higher or lower (close to zero) importance of winter precipitation conditions (Figure 3). That we did not see

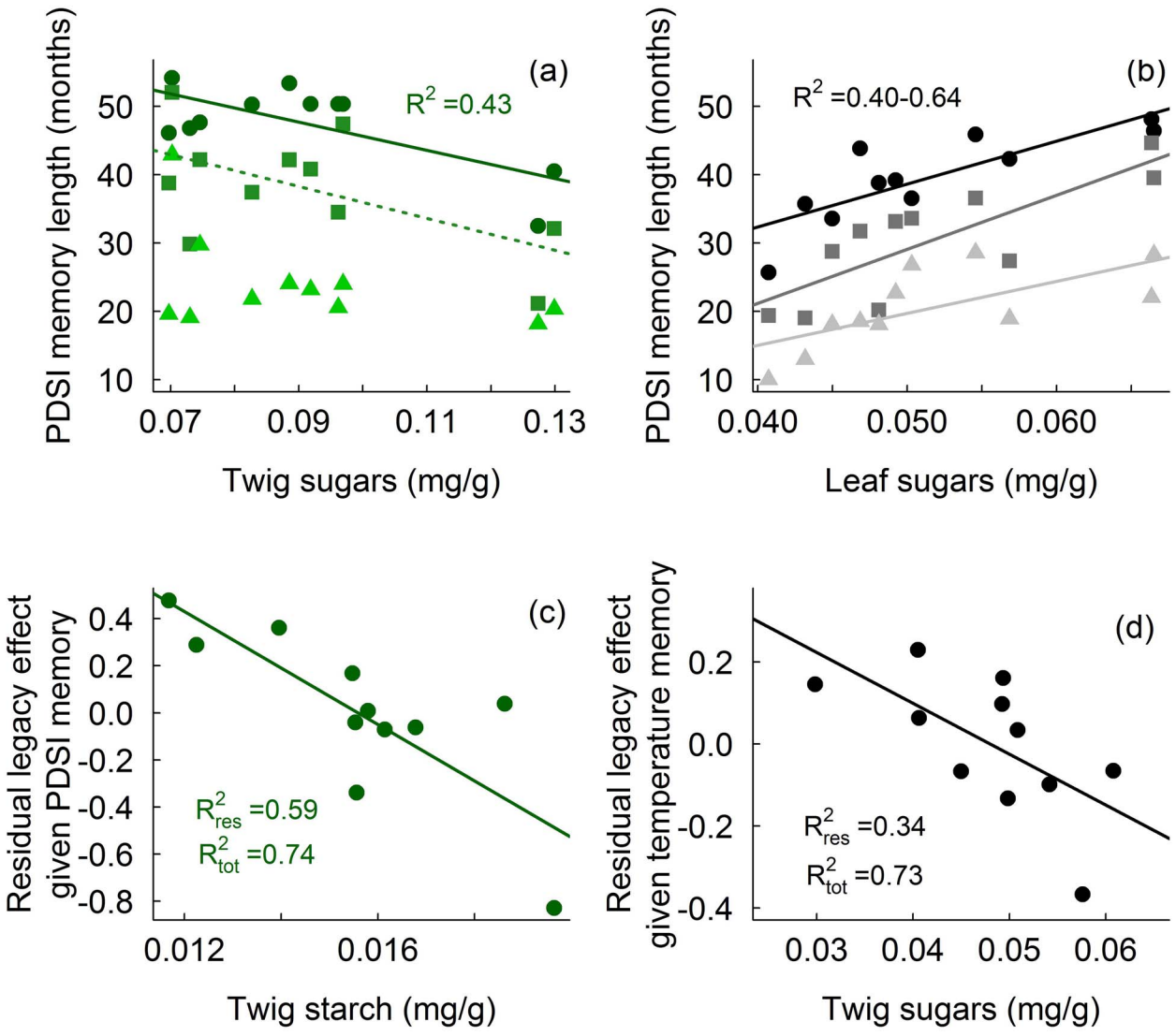

Figure 5. Variation in memory length and drought legacies across sites are related to NSC concentrations in aspen (green colors; a, c) and piñon (black colors; b, d). PDSI memory length (e.g., M^{50} = triangles, M^{75} = squares and M^{90} = circles) is related to sugar concentrations in (a) aspen twigs and (b) piñon leaves, but the sign differs (*implicit effects*) such that memory decreases with increasing sugars in aspen, but the opposite relationship occurs for piñon. After accounting for the effect of (c) PDSI memory length in aspen or (d) temperature memory length in piñon on the legacy effects of recent droughts, NSC concentrations explain additional variation in drought legacies (*additive effects*). Solid lines signify significant linear regressions ($P < 0.05$) and dashed lines indicate marginal relationships ($0.05 < P < 0.1$). In (c, d), R^2 of both the residual regressions (after accounting for memory length) and total regressions (including memory length) are reported.

similar variation is juniper is likely because we were only able to accurately crossdate sites ($n = 4$ sites) that had similar climate sensitivity to co-occurring piñon (Table 1). Because we attempted to select representative trees at each site and did not limit our selection to very old, isolated individuals, these results may reflect this more 'ecological' tree-ring sampling strategy (Nehrbass-Ahles et al. 2014). We found no evidence for systematic spatial variability in either climate sensitivity or memory, perhaps due to the complex climatological controls on moisture and heat stress in the southwestern USA (Douglas et al. 1993, Szejner et al. 2016).

Implications of variation in memory across species

Clear differences in the climate memory of tree growth across species did emerge, which may be related to broad differences in NSC storage between gymnosperms and angiosperms (Hoch et al. 2003). The precipitation and PDSI memories were longer in aspen compared to the two conifer species, while temperature memory was more similar across species (Figure 4a-c). Some portion of the climate memory of growth is likely driven by multi-year storage and remobilization of NSCs (Kozlowski 1992, Carbone et al. 2013, Ogle et al. 2015), and because angiosperms tend to have higher NSC concentrations

in many tissues, particularly wood (Hoch et al. 2003), this could underlie comparatively longer memory of moisture-related climate conditions in aspen. In general, climatic memory may have been influenced by NSC storage across seasons, years and decades, but also likely snowmelt dynamics, particularly in the southern Rockies in the western USA (Truettner et al. 2018, Love et al. 2019). Though, repeated cavitation of the stem xylem and carbon allocation dynamics also probably induce lagged growth responses to climate (Trugman et al. 2018, Kannenberg et al. 2019). The temporal patterns in memory observed for piñon and juniper are well documented (Peltier et al. 2018) and consistent with a deep body of dendrochronology literature in the southwestern USA (Fritts 1976). In contrast, the climate sensitivity and memory of aspen is comparatively poorly quantified, though recent work has shown aspen growth to be limited under warm and dry conditions (Ireland et al. 2020). Longer precipitation memory in aspen could emerge from more mesic climate conditions experienced in mixed conifer forests where these trees occur, or relatively greater NSC concentrations (Peltier et al. 2020). Aspen trees in this study were also less sensitive to precipitation on average compared to piñon and juniper (Figure 2a), and were perhaps buffered by more mesic conditions, or hillslope hydrology leading to multi-year soil moisture storage (Rempe and Dietrich 2018, Love et al. 2019).

Long climate memory does not necessarily confer drought resilience

Across species, climatic memory could confer some benefits to trees: by integrating climate responses across multiple seasons and years, memory allows trees to grow in response to reduced 'perceived' variation in climatic conditions (Figure S5 available as Supplementary data at *Tree Physiology* Online). That is, trees with longer memory might be less impacted by transient droughts because growth is driven by precipitation conditions experienced over multiple years. While this expectation—greater drought resilience in trees with longer climate memory—seems supported in piñon, relationships among memory and drought legacies in aspen suggest long memory of temperature can instead negatively impact post-drought growth (Table 2). Notable for both species was the absence of correlations between drought legacies and precipitation memory indices. Temperature memory best explained variation in drought legacies across our study sites, consistent with a major role of heat stress via VPD in contemporary drought in the western USA. That is, while recent (post-2000) conditions may not be exceptionally dry compared to paleo-climate records, they are very clearly exceptionally warm (Williams et al. 2013, 2020, Cook et al. 2014; Figure 1d), and this additional VPD stress may drive additional stomatal limitations. Here, the length of temperature memory in piñon was associated with relatively lower post-drought impacts (less negative legacies; Table 2). However, the opposite was true for aspen, where growth at sites with longer temperature memory tended to be more over-predicted by the model following the 2011–2012 drought (Table 2). In piñon, these results suggest simply that sites with longer temperature memory are buffered from transient temperature extremes that often coincide with drought events.

In contrast, the relationship quantified for aspen could suggest lasting negative impacts of warmer conditions at sites where trees have longer memory of temperature conditions, perhaps related to lasting hydraulic damage. Aspen occurs in higher elevation, more mesic forests, and there is evidence that aspen is poorly adapted to regulate water loss during recent drought events (Anderegg et al. 2012). While there is some evidence for the ability to repair embolism in this species (Love and Sperry 2018), complete recovery of hydraulic function is unlikely given evidence of widespread cavitation fatigue and multi-year hydraulic deterioration (Anderegg et al. 2013, 2014). Additionally, drought may also deplete NSC reserves and deep soil moisture resources, and may exacerbate existing negative impacts of pre-existing insect pests or fungal pathogens (Manion 1991, Voelker et al. 2008). Larger prediction errors (i.e., more negative drought legacies, d^*_{yr}) following the 2011–2012 drought at aspen sites with long temperature memory could also suggest that rather than precipitation, temperature conditions (or temperature controls on precipitation response, via PDSI) tend to govern recovery from drought in this species. In a global synthesis of carbon flux data, post-drought temperature extremes were found to be more influential than low precipitation in modulating post-drought recovery (Schwalm et al. 2017).

Legacy-NSC relationships reflect multiple functions of NSC

While some studies have explored drought recovery in pot experiments or lysimeters with seedlings or saplings (O'Brien et al. 2014, Hagedorn et al. 2016, Sapes et al. 2019, Kannenberg and Phillips 2020), this is the first study to explore the relationships between the temporal characteristics of tree growth and drought recovery with variation in snapshot measurements of NSC concentrations in mature trees. NSC concentrations were measured in 2016, so relationships among these 'snapshot' physiological measurements and indices of climatic memory and multi-year drought legacies may seem surprising (Figure 5). In this study, we consider the relevant variability in NSC concentrations here to indicate broad differences in carbon allocation strategies (perhaps genetically driven [Blonder et al. 2020, Godfrey et al. 2020, Blumstein and Hopkins 2021], mean climate conditions (as they influence carbohydrate supply or sink strength, e.g., growth, but also osmoregulation (Piper et al. 2017)), or maximum NSC storage capacity (Hoch et al. 2003) across sites. Differences in storage capacity may themselves

covary with climate, driven perhaps by wood anatomical features and investments in structural vs. storage tissues. While some proportion of the variability in NSC's likely reflects recent climate conditions (including the preceding drought event Peltier et al. 2020), short-term variability is of course unrelated to quantities describing tree growth over years to decades (i.e., drought legacies and climatic memory).

This may be why significant relationships between memory or legacies and NSC were nearly exclusively related to NSC pools in twigs (rather than leaves; Figure 5). Leaf NSC pools are more likely to reflect short-term (fast) fluctuations in carbon supply following recent moisture and temperature conditions. Using similar logic, one might expect to find primarily relationships with starch pools, as sugar concentrations have in the past been conceptualized to reflect 'fast' dynamics (Dietze et al. 2014). However, we found significant relationships with sugar and starch concentrations, pointing towards regulation of osmotic potentials as a key functional role of sugars (Guo et al. 2020), or at least a pool of carbohydrates that is significantly modulated by climate conditions. That this was related to climate variation suggests trees are locally adapted to their climate via osmoregulatory mechanisms, where trees at lower elevations or hotter, drier sites may store more sugars in twig tissues (Lintunen et al. 2016, Piper et al. 2017, Godfrey et al. 2020). In the southwestern USA, perhaps due to the influence of the North American Monsoon, we did not find clear patterns in NSC pool sizes across elevations or sites that were clearly related to climate (results not shown).

Conclusion

Strong relationships between growth and NSC concentrations suggests that differences in tree carbon allocation are broadly detectable across sites, and that carbon allocation priorities (such as growth, respiration, osmoregulation or starch storage in twigs) can influence tree-ring width responses to climate across long time scales. We argue that climatic memory of tree growth is a critical property of the tree growth response to climate across species (Peltier et al. 2018), where for example, accounting for memory can influence predictions of drought recovery (Peltier and Ogle 2019*a*, 2019*b*). Here, after accounting for climate memory, much of the site variation in post-drought prediction error can be explained by variation in memory length and NSC concentrations. Future work to improve our understanding of the mechanistic links between physiological traits and the temporal characteristics of tree growth should focus on generating physiological time series over multiple years, particularly focused on climate extremes. These types of datasets will improve our understanding of the physiological processes driving the memory of tree growth and the legacy effects of extreme climate events such as severe droughts.

Author contributions

K.O., W.R.L.A., G.W.K., M.E.L., C.S., D.A. and J.D.S. conceived of the overarching study goals and sampling plan. K.S.C., J.D.S. and K.O. selected field sites. D.M.P.P., J.G., P.N., M.B., M.W., K.S.C., L.L.Y., Y.L., M.K.F., G.W.K. and K.O. collected the data. L.L.Y. led the tree-ring crossdating. K.O. and D.M.P.P. conceived of and conducted the statistical analysis. D.M.P.P. wrote the first draft of the manuscript with substantial input from K.O., J.D.S., L.L.Y. and K.S.C.

Supplementary data

Supplementary data for this article are available at *Tree Physiology* Online.

Acknowledgments

This work was funded by an NSF-DEB RAPID grant #1643245 and an NSF-ABI grant #1458867.

Data availability statement

If accepted, code will be archived in Zenodo. Tree ring chronologies will be uploaded to the International Tree Ring Data Bank.

References

Abatzoglou JT, McEvoy DJ, Redmond KT (2017) The west wide drought tracker: drought monitoring at fine spatial scales. Bull Am Meteorol Soc 98:1815–1820.

Anderegg WR, Anderegg LD, Berry JA, Field CB (2014) Loss of whole-tree hydraulic conductance during severe drought and multi-year forest die-off. Oecologia 175:11–23.

Anderegg WR, Anderegg LD, Huang C (2019) Testing early warning metrics for drought-induced tree physiological stress and mortality. Glob Chang Biol 25:2459–2469.

Anderegg WR, Plavcová L, Anderegg LD, Hacke UG, Berry JA, Field CB (2013) Drought's legacy: multiyear hydraulic deterioration underlies widespread aspen forest die-off and portends increased future risk. Glob Chang Biol 19:1188–1196.

Anderegg WRL, Berry JA, Smith DD, Sperry JS, Anderegg LDL, Field CB (2012) The roles of hydraulic and carbon stress in a widespread climate-induced forest die-off. Proc Natl Acad Sci 109:233–237.

Anderegg WRL, Schwalm C, Biondi F et al. (2015) Pervasive drought legacies in forest ecosystems and their implications for carbon cycle models. Science 349:528–532.

Babst F, Bouriaud O, Papale D et al. (2014) Above-ground woody carbon sequestration measured from tree rings is coherent with net ecosystem productivity at five eddy-covariance sites. New Phytol 201:1289–1303.

Blonder B, Graae BJ, Greer B et al. (2020) Remote sensing of ploidy level in quaking aspen (*Populus tremuloides* Michx.). J Ecol 108:175–188.

Blumstein M, Hopkins R (2021) Adaptive variation and plasticity in non-structural carbohydrate storage in a temperate tree species. Plant Cell Environ 0:1–12.

Bond-Lamberty B, Rocha AV, Calvin K, Holmes B, Wang C, Goulden ML (2014) Disturbance legacies and climate jointly drive tree growth and mortality in an intensively studied boreal forest. Glob Chang Biol 20:216–227.

Bunn AG (2008) A dendrochronology program library in R (dplR). Dendrochronologia 26:115–124.

Carbone MS, Czimczik CI, Keenan TF, Murakami PF, Pederson N, Schaberg PG, Xu X, Richardson AD (2013) Age, allocation and availability of nonstructural carbon in mature red maple trees. New Phytol 200:1145–1155.

Cook BI, Smerdon JE, Seager R, Cook ER (2014) Pan-continental droughts in North America over the last millennium. J Climate 27:383–397.

Dietze MC, Sala A, Carbone MS, Czimczik CI, Mantooth JA, Richardson AD, Vargas R (2014) Nonstructural carbon in woody plants. Annu Rev Plant Biol 65:667–687.

Douglas MW, Maddox RA, Howard K, Reyes S (1993) The Mexican monsoon. J Climate 6:1665–1677.

Esper J, Frank D (2009) Divergence pitfalls in tree-ring research. Clim Change 94:261–266.

Fritts HC (1976) Tree rings and climate. Academic Press, San Diego, California, p. 567.

Fritts HC, Smith DG, Cardis JW, Budelsky CA (1965) Tree-ring characteristics along a vegetation gradient in northern Arizona. Ecology 46:394–401.

Fritts HC, Swetnam TW (1989) Dendroecology: a tool for evaluating. Adv Ecol Res 19:111–188.

Godfrey JM, Riggio J, Orozco J, Guzmán-Delgado P, Chin AR, Zwieniecki MA (2020) Ray fractions and carbohydrate dynamics of tree species along a 2750 m elevation gradient indicate climate response, not spatial storage limitation. New Phytol 225:2314–2330.

Guo JS, Gear L, Hultine KR, Koch GW, Ogle K (2020) Non-structural carbohydrate dynamics associated with antecedent stem water potential and air temperature in a dominant desert shrub. Plant Cell Environ 43:1467–1483.

Hagedorn F, Joseph J, Peter M et al. (2016) Recovery of trees from drought depends on belowground sink control. Nature Plants 2:16111.

Hoch G, Richter A, Körner C (2003) Non-structural carbon compounds in temperate forest trees. Plant Cell Environ 26:1067–1081.

Ireland KB, Moore MM, Fulé PZ, Yocom L, Zegler TJ (2020) Warm, dry conditions inhibit aspen growth, but tree growth and size predict mortality risk in the southwestern United States. Can J For Res 50:1206–1214.

Kannenberg SA, Novick KA, Alexander MR, Maxwell JT, Moore DJP, Phillips RP, Anderegg WRL (2019) Linking drought legacy effects across scales: from leaves to tree rings to ecosystems. Glob Chang Biol 5:2978–2992.

Kannenberg SA, Phillips RP (2020) Non-structural carbohydrate pools not linked to hydraulic strategies or carbon supply in tree saplings during severe drought and subsequent recovery. Tree Physiol 40:259–271.

Kannenberg SA, Schwalm CR, Anderegg WRL (2020) Ghosts of the past: how drought legacy effects shape forest functioning and carbon cycling. Ecol Lett 23:891–901.

Klesse S, DeRose RJ, Babst F, Black B, Anderegg LDL, Axelson J, Ettinger A, Griesbauer H, Guiterman CH, Harley G (2020) Continental-scale tree-ring based projection of Douglas-fir growth–testing the limits of space-for-time substitution. Glob Chang Biol 26:5146–5163.

Knowles JF, Scott RL, Biederman JA, Blanken PD, Burns SP, Dore S, Kolb TE, Litvak ME, Barron-Gafford GA (2020) Montane forest productivity across a semi-arid climatic gradient. Glob Chang Biol 26:6945–6958.

Kozlowski TT (1992) Carbohydrate sources and sinks in woody plants. Botanical Rev 58:107–222.

LaMarche VC Jr, Stockton CW (1974) Chronologies from temperature-sensitive bristlecone pines at upper treeline in western United States. Tree-Ring Bulletin 374:21–44.

Landhäusser SM, Chow PS, Dickman LT, Furze ME, Kuhlman I, Schmid S, Wiesenbauer J, Wild B, Gleixner G, Hartmann H (2018) Standardized protocols and procedures can precisely and accurately quantify non-structural carbohydrates. Tree Physiol 38: 1764–1778.

Lintunen A, Paljakka T, Jyske T, Peltoniemi M, Sterck F, Von Arx G, Cochard H, Copini P, Caldeira MC, Delzon S (2016) Osmolality and non-structural carbohydrate composition in the secondary phloem of trees across a latitudinal gradient in Europe. Front Plant Sci 7:726.

Liu Y, Schwalm CR, Samuels-Crow KE, Ogle K (2019) Ecological memory of daily carbon exchange across the globe and its importance in drylands. Ecol Lett 22:1806–1816.

Love DM, Sperry JS (2018) In situ embolism induction reveals vessel refilling in a natural aspen stand. Tree Physiol 38: 1006–1015.

Love DM, Venturas MD, Sperry JS, Brooks PD, Pettit JL, Wang Y, Anderegg WRL, Tai X, Mackay DS (2019) Dependence of aspen stands on a subsurface water subsidy: Implications for climate change impacts. Water Resour Res 55:1833–1848.

Makinen H, Nojd P, Mielikainen K (2000) Climatic signal in annual growth variation of Norway spruce (*Picea abies*) along a transect from Central Finland to the Arctic timberline. Can J For Res 30: 769–777.

Manion P (1991) Tree disease concepts, 2nd edn. Prentice-Hall, Upper Saddle River, NJ, USA.

Marquardt PE, Miranda BR, Jennings S, Thurston G, Telewski FW (2018) Variable climate response differentiates the growth of Sky Island ponderosa pines. Trees 33:317–332.

Mazza G, Manetti MC (2013) Growth rate and climate responses of *Pinus pinea* L. in Italian coastal stands over the last century. Clim Change 121:713–725.

Melvin TM, Briffa KR (2008) A "signal-free" approach to dendroclimatic standardisation. Dendrochronologia 26:71–86.

Nehrbass-Ahles C, Babst F, Klesse S, Nötzli M, Bouriaud O, Neukom R, Dobbertin M, Frank D (2014) The influence of sampling design on tree-ring-based quantification of forest growth. Glob Chang Biol 20:2867–2885.

O'Brien MJ, Leuzinger S, Philipson CD, Tay J, Hector A (2014) Drought survival of tropical tree seedlings enhanced by non-structural carbohydrate levels. Nature Climate Change 4:710–714.

Ogle K, Barber JJ, Barron-Gafford GA, Bentley LP, Cable JM, Huxman TE, Loik ME, Tissue DT (2015) Quantifying ecological memory in plant and ecosystem processes. Ecol Lett 18:221–235.

Pan Y, Birdsey RA, Fang J et al. (2011) A large and persistent carbon sink in the world's forests. Science 333:988–993.

Pederson N, Leland C, Bishop DA, Pearl JK, Anchukaitis KJ, Mandra T, Hopton-Ahmed M, Martin-Benito D (2020) A framework for determining population-level vulnerability to climate: evidence for growth hysteresis in *Chamaecyparis thyoides* along its contiguous latitudinal distribution. Front For Global Change 3:39.

Peltier DM, Ogle K (2019a) Legacies of La Niña: north American monsoon can rescue trees from winter drought. Glob Chang Biol 25:121–133.

Peltier DM, Ogle K (2020) Tree growth sensitivity to climate is temporally variable. Ecol Lett 23:1561–1572.

Peltier DMP, Barber JJ, Ogle K (2018) Quantifying antecedent climatic drivers of tree growth in the Southwestern US. J Ecol 106: 613–624.

Peltier DMP, Fell M, Ogle K (2016) Legacy effects of drought in the southwestern United States: a multi-species synthesis. Ecological Monographs 86:312–326.

Peltier DMP, Guo JS, Nguyen P et al. (2020) Temporal controls on crown non-structural carbohydrates in southwestern US tree species. Tree Physiol 41:388–402.

Peltier DMP, Ogle K (2019b) Legacies of more frequent drought in ponderosa pine across the western United States. Glob Chang Biol 25:3803–3816.

Pérez-Ramos IM, Ourcival JM, Limousin JM, Rambal S (2010) Mast seeding under increasing drought: results from a long-term data set and from a rainfall exclusion experiment. Ecology 91: 3057–3068.

Piper FI, Fajardo A, Hoch G (2017) Single-provenance mature conifers show higher non-structural carbohydrate storage and reduced growth in a drier location. Tree Physiol 37:1001–1010.

Plummer M (2013) rjags: Bayesian graphical models using MCMC, R package version 3–10. Workshop on Distributed Statistical Computing, Vienna, p 125.

Plummer M (2003) JAGS: a program for analysis of Bayesian graphical models using Gibbs sampling. Proceedings of the 3rd International Workshop on Distributed Statistical Computing, 124:125.

PRISM Climate Group, Oregon State University, http://prism.oregonstate.edu, created 4 Feb 2004.

Quentin AG, Pinkard EA, Ryan MG et al. (2015) Non-structural carbohydrates in woody plants compared among laboratories. Tree Physiol 35:1146–1165.

R Core Team (2019) R: a language and environment for statistical computing, Vol. 2019. R Foundation for Statistical Computing.

Rempe DM, Dietrich WE (2018) Direct observations of rock moisture, a hidden component of the hydrologic cycle. Proceedings of the National Academy of Sciences 115:2264–2669.

Ryan EM, Ogle K, Zelikova TJ, LeCain DR, Williams DG, Morgan JA, Pendall E (2015) Antecedent moisture and temperature conditions modulate the response of ecosystem respiration to elevated CO2 and warming. Glob Chang Biol 21:2588–2602.

Sapes G, Roskilly B, Dobrowski S, Maneta M, Anderegg WR, Martinez-Vilalta J, Sala A (2019) Plant water content integrates hydraulics and carbon depletion to predict drought-induced seedling mortality. Tree Physiol 39:1300–1312.

Sarris D, Christodoulakis D, Körner C (2007) Recent decline in precipitation and tree growth in the eastern Mediterranean. Glob Chang Biol 13:1187–1200.

Schwalm CR, Anderegg WR, Michalak AM et al. (2017) Global patterns of drought recovery. Nature 548:202–205.

Szejner P, Wright WE, Babst F, Belmecheri S, Trouet V, Leavitt SW, Ehleringer JR, Monson RK (2016) Latitudinal gradients in tree ring stable carbon and oxygen isotopes reveal differential climate influences of the north American monsoon system. J Geophys Res Biogeo 121:1978–1991.

Truettner C, Anderegg WRL, Biondi F, Koch GW, Ogle K, Schwalm C, Litvak ME, Shaw JD, Ziaco E (2018) Conifer radial growth response to recent seasonal warming and drought from the southwestern USA. For Ecol Manage 418:55–62.

Trugman AT, Detto M, Bartlett MK, Medvigy D, Anderegg WRL, Schwalm C, Schaffer B, Pacala SW (2018) Tree carbon allocation explains forest drought-kill and recovery patterns. Ecol Lett 21: 1552–1560.

Vacchiano G, Hacket-Pain A, Turco M, Motta R, Maringer J, Conedera M, Drobyshev I, Ascoli D (2017) Spatial patterns and broad-scale weather cues of beech mast seeding in Europe. New Phytol 215:595–608.

Voelker SL, Muzika R-M, Guyette RP (2008) Individual tree and stand level influences on the growth, vigor, and decline of red oaks in the Ozarks. Forest Science 54:8–20.

von Arx G, Arzac A, Fonti P, Frank D, Zweifel R, Rigling A, Galiano L, Gessler A, Olano JM (2017) Responses of sapwood ray parenchyma and non-structural carbohydrates of *Pinus sylvestris* to drought and long-term irrigation. Funct Ecol 31:1371–1382.

Williams AP, Allen CD, Macalady AK et al. (2013) Temperature as a potent driver of regional forest drought stress and tree mortality. Nat Climate Change 3:292–297.

Williams AP, Cook ER, Smerdon JE, Cook BI, Abatzoglou JT, Bolles K, Baek SH, Badger AM, Livneh B (2020) Large contribution from anthropogenic warming to an emerging north American megadrought. Science 368:314–318.

Zweifel R, Etzold S, Sterck F, Gessler A, Anfodillo T, Mencuccini M, von Arx G, Lazzarin M, Haeni M, Feichtinger L (2020) Determinants of legacy effects in pine trees–implications from an irrigation-stop experiment. New Phytol 227:1081–1096.